Video Article

Establishment of a Segmental Femoral Critical-size Defect Model in Mice Stabilized by Plate Osteosynthesis

Mathieu Manassero[1,2], Adeline Decambron[1,2], Bui Truong Huu Thong[1], Véronique Viateau[1,2], Morad Bensidhoum[1], Hervé Petite[1]

[1]Laboratoire de Bioingénierie et Biomécanique Ostéo-Articulaires (B2OA - UMR CNRS 7052), Université Paris Diderot

[2]Ecole Nationale Vétérinaire d'Alfort, Université Paris-Est

Correspondence to: Hervé Petite at herve.petite@univ-paris-diderot.fr

URL: http://www.jove.com/video/52940
DOI: doi:10.3791/52940

Keywords: Medicine, Issue 116, bone, mice, plate osteosynthesis, defect, bone isograft, coral, tissue engineering, bone construct, animal models, bone formation, bone repair

Date Published: 10/12/2016

Citation: Manassero, M., Decambron, A., Huu Thong, B.T., Viateau, V., Bensidhoum, M., Petite, H. Establishment of a Segmental Femoral Critical-size Defect Model in Mice Stabilized by Plate Osteosynthesis. *J. Vis. Exp.* (116), e52940, doi:10.3791/52940 (2016).

Abstract

The use of tissue-engineered bone constructs is an appealing strategy to overcome drawbacks of autografts for the treatment of massive bone defects. As a model organism, the mouse has already been widely used in bone-related research. Large diaphyseal bone defect models in mice, however, are sparse and often use bone fixation which fills the bone marrow cavity and does not provide optimal mechanical stability. The objectives of the current study were to develop a critical-size, segmental, femoral defect in nude mice. A 3.5-mm mid-diaphyseal femoral ostectomy (approximately 25% of the femur length) was performed using a dedicated jig, and was stabilized with an anterior located locking plate and 4 locking screws. The bone defect was subsequently either left empty or filled with a bone substitute (syngenic bone graft or coralline scaffold). Bone healing was monitored noninvasively using radiography and *in vivo* micro-computed-tomography and was subsequently assessed by *ex vivo* micro-computed-tomography and undecalcified histology after animal sacrifice, 10 weeks postoperatively. The recovery of all mice was excellent, a full-weight-bearing was observed within one day following the surgical procedure. Furthermore, stable bone fixation and consistent fixation of the implanted materials were achieved in all animals tested throughout the study. When the bone defects were left empty, non-union was consistently obtained. In contrast, when the bone defects were filled with syngenic bone grafts, bone union was always observed. When the bone defects were filled with coralline scaffolds, newly-formed bone was observed in the interface between bone resection edges and the scaffold, as well as within a short distance within the scaffold.

The present model describes a reproducible critical-size femoral defect stabilized by plate osteosynthesis with low morbidity in mice. The new load-bearing segmental bone defect model could be useful for studying the underlying mechanisms in bone regeneration pertinent to orthopaedic applications.

Video Link

The video component of this article can be found at http://www.jove.com/video/52940/

Introduction

Massive diaphyseal bone defects are a great challenge to the orthopaedic surgeon. Bone replacement with autologous bone graft, currently considered as the gold-standard treatment, is in limited supply and is associated with harvesting-related morbidity. For these reasons, tissue-engineered bone constructs combining bone marrow mesenchymal stem cells with osteoconductive scaffolds have been explored as an alternative for autografts in orthopaedic surgery.

To date, most of the studies have been performed in clinically-relevant animal models such as dogs, pigs and sheep[1-3], but preliminary evaluation of these constructs in orthotopic, segmental, critical-size bone defects in small-animal models (like mice) could have several advantages: (i) low expenses, (ii) large numbers of animals can be operated; (iii) in contrast to large animal models, homogeneity of the mouse strains limits individual variations in scaffold resorption and bone formation and; (iv) most importantly, availability of specific antibodies and gene-targeted animals enable the evaluation of the biological process involved in bone healing. Last but not least, use of immunodeficient strains of mice also enables studies using either grafts or cells of human origin without adverse immune responses in mice.

Despite the aforementioned advantages, massive diaphyseal bone defect models in mice are sparse. Most of such models use bone fixation with an intramedullary pin which fills the bone marrow cavity (thus limiting the volume of material to be tested) and also impedes reproducibility by not providing rotational and axial stability[2,4-7].

The objectives of the current study are (i) mimicking a clinical bone non-union situation, to describe a reproducible, critical-size, segmental, femoral defect model in mice, which is stabilized by accurate and reproducible locking-plate osteosynthesis that provides a highly stable

biomechanical environment[8-10]; (ii) to illustrate the present model with two potential bone substitutes and to describe bone formation analyses that could be used.

Protocol

Ethics Statement: The mice used in the present study were treated in accordance with the guidelines published by the European Committee for "Care and Use of Laboratory Animals" (Directive 2010/63/EU and the European Convention ETS 123). The experimental protocol was approved by the Ethics Committee of the Faculty of Medicine Lariboisière Saint-Louis (CEEA LV/2010-01-04).

1. Animals

1. Use athymic mice (10 weeks old). Use a minimal number of 6 mice with defect left empty as negative control group.

2. Scaffolds Preparation

1. **Syngenic Graft Preparation**
    1. Use bone isograft to fill the defect to provide control group with a minimum number of 6 animals.
    2. Obtain bone isografts by harvesting excised femoral bone from mouse belonging to either "defects left empty or "defects filled with coral scaffold" groups (this avoids the use of extra animal to collect bone isograft)[11].
    3. Flush the resected bone with Phosphate Buffered Saline (PBS) and keep it sterile using moist gauze compress.

2. **Coral Scaffold Preparation**
    1. Use scaffold that are made of natural coral: *Acropora* sp. coral exoskeleton cubes, 3 x 3 x 3 mm as potential bone substitute with a minimum of 6 animals.
    2. Carve by hand each coral cube to the shape of cylinder (3.5 height; 2 mm diameter).
    3. Sterilize each scaffold by autoclaving (121 °C for 20 min), wash it with sterile PBS, and immersed it in complete culture medium (α-MEM) for 24 hr before implantation in mice.

3. Anesthetic Procedures and Analgesia

1. Provide preventive analgesia, 15 min prior to anesthesia, by subcutaneous injection of buprenorphine (0.1 mg/kg animal body weight).
2. Apply ointment in the animal eyes to prevent dryness every 30 min while the animals are under anesthesia.
3. Place the mice on a warming pad to prevent hypothermia.
4. **Anesthesia and Analgesia during the Surgical Procedure**
    1. Inject intraperitoneally a solution containing xylazine (8 mg/kg) and ketamine (100 mg/kg).
    2. Deliver oxygen *via* flow-by (50 ml/min).
    3. Confirm adequate depth of anesthesia by the presence of good muscle relaxation and lack of animal response to a noxious stimulus (*e.g.*, firm toe pinch).
    4. Inject subcutaneously a single dose of enrofloxacin (0.05 mg/kg) as microbial prophylaxis.

5. **Post-operative Analgesia**
    1. Provide postoperative analgesia by subcutaneous injection of buprenorphine (0.1 mg/kg) every 12 hr for 3 consecutive days.

6. **Anesthesia during Diagnostic Imaging Procedures**
    1. Place the mice in an anesthetizing-box, and then induce and maintain anesthesia using approximately 4% and 2% isoflurane in oxygen, respectively.
    2. Confirm adequate depth of anesthesia by good animal muscle relaxation and the lack of movement.

7. **Recovery Conditions**
    1. Keep the mice on warming pad until full recovery
    2. Do not leave an animal unattended until it has regained sufficient consciousness to maintain sternal recumbency after surgery.
    3. Do not return an animal that has undergone surgery to the company of other animals until fully recovered.

8. **Post-operative Conditions**
    1. Host the mice separately during the first 3 days Host the mice by 4 in cages after day 3.
    2. Provide water and adapted food *ad libitum*. Allow the mice to weight-bear, without any activity restriction throughout the post-operative period.

4. Surgical procedure: Femoral Segmental Defect Model[11,12]

1. After anesthesia, place each mouse in ventral recumbency with the left hind limb in extension.
2. Scrub the limb for aseptic surgery using 10% povidone iodine for 5 min and then place a sterile drape under the limb to create a sterile surface (a sterile transparent drape is used in order to be able to monitor respiratory movement during the procedure). Care is taken to maintain sterility of the surgical field during the procedure.
3. Make a 15 - 17-mm longitudinal skin incision over the anterolateral aspect of the femur, extending from the hip joint to the stifle joint.

4. Incise the *fascia lata*, split the *vastus lateralis* muscle and the *biceps femoris* muscle to expose the full length of the femoral diaphysis. Caution should be taken to preserve the sciatic nerve caudally and the articular capsule distally (**Figure 1**).
5. To enhance femoral diaphysis exposure, transect the *gluteal muscle* and *biceps femoris* from the 3rd trochanter.
6. Perform a circular dissection of the femur at the middle of the diaphysis.
7. Apply a 6-hole titanium micro-locking plate (10 mm long; 1.5 mm wide, weight: 30 mg) on the anterior femoral side.
   NOTE: The holes of the plate, which are conically recessed with a cylindrical portion, accommodate titanium self-tapping locking screws (2 mm long, 0.47 mm outer diameter, weight: 5 mg, with undersurface of the head screw threaded to enable locking within the plate hole) that are connected to a stem, which twists off when locked.
8. Drill the most proximal hole of the plate using a 0.3 mm drill bit and either dedicated engine power or non-dedicated engine power operated at 2,500 rpm at approximately 500 mW[12]).
9. Insert the first screw using a dedicated screwdriver and then lock it (**Figure 2**).
   NOTE: Since alignment of the plate is determined by application of this first screw, it is important to position the plate parallel to the femur when inserting the screw.
10. Drill the most distal hole of the plate in a similar fashion, insert and lock the screw (**Figure 3**).
11. Insert, but do no lock, the two other outer screws.
12. Place the wire of the 0.22 mm Gigli saw closely around the bone in a medio-lateral orientation and then insert it in the slots of the jig (**Figure 4**).
13. Insert the dedicated jig on the stem of the two last screws and apply it above the plate (**Figure 5**).
14. Perform a 3.5-mm long mid-diaphyseal femoral ostectomy using the Gigli saw under irrigation (using sterile isotonic saline) to prevent thermal necrosis. Have the surgeon's assistant take the jig. Have the surgeon apply a constant steady tension. Be careful not to tangle the saw wire and to use the middle two-thirds of the wire. Avoid excess movement in order to obtain a straight bone cut (**Figure 6**).
15. After the ostectomy, remove the Gigli saw. To avoid damage of the soft tissue, cut the saw wire close to the bone on one side.
16. Remove the jig and lock the two last screws (**Figure 7**).
17. Either leave the segmental defect empty or surgically fill it by putting materials to be tested inside the defect.
18. Copiously rinse the surgical field with sterile isotonic saline.
19. Place the *vastus lateralis* muscle loosely over the plate. Close the fascia and subcutaneous planes using a simple continuous suture pattern and 5.0 glycomer 631 suture; close the skin with a simple interrupted suture pattern using 4.0 glycomer 631 suture. Alternatively, it is also possible to close the skin using skin glue.

5. *In Vivo* Assessments of Bone Regeneration

1. With the mice under anesthesia, perform radiographic assessments in a longitudinal manner using both conventional X-rays (26 kV, 10 sec; 2X magnification; 20 lines/mm spatial resolution) and high-resolution micro-computed tomography (µCT).
2. For µCT analysis, acquire images at a resolution of 36 µm (50 kV and 478 mA, at 40 msec exposure time, using a 0.5 mm aluminum filter, rotation step of 0.7**º**, and tomographic rotation of 180**º**). Analyze the images using the resident software.

6. *Ex Vivo* Assessments of Bone Regeneration

1. Ten weeks after surgery, induce anesthesia using isoflurane in oxygen, and then sacrifice the mice by intraperitoneal injection of an overdose of barbiturate (1 ml of pentobarbital).
2. Excise the femoral bones, remove overlaying muscle tissue, and fix the bone specimens in 4% paraformaldehyde (pH 7.4) for four days.
3. Remove the plate and screws from each excised bone specimen after paraformaldehyde fixation.
4. ***Ex Vivo* µCT Analysis**
   1. Place each excised and fixed bone in polyethylene tubes filled with 75% alcohol and analyze it using *ex vivo* µCT.
   2. Acquire images at 80 kV and 100 µA (exposure time of 1,000 msec, aluminum 0.5 filter, and 4 µm camera pixel size (2,400 x 4,000 with a voxel size of 7 µm), average four frames for each rotation increment of 0.9**º**.
   3. Reconstruct 3-dimensional images (average voxel size of 13 µm) using a Hamming-filtered back-projection with the resident software.
   4. For quantitative analysis of bone formation, use resident software to obtain the volume of mineralized tissue (lower grey threshold of 45 grayscale indices and upper grey threshold of 240 grayscale indices) in a determined and consistent region of interest corresponding to the defect.
   5. Perform analyses in the same manner for each mouse with the same region of interest.
   6. Use the one-way analysis test (confidence interval - at 95% and the significant level at $p < 0.05$) to compare the bone union rate and the volume of mineralized tissue in the region of interest between groups.

5. **Histological Analysis**
   1. Embed each excised and fixed femoral bone in methyl methacrylate resin and process it for undecalcified histology.
   2. Cut each bone specimen lengthwise into thick section (200 µm) using a circular water-cooled diamond saw.
   3. Grind each bone specimen section down to a thickness of 100 µm, polish it, and stain it using Stevenel blue and van Gieson picrofuchsin stains.
      NOTE: After staining, cells appear in blue, bone in pink, and coral in brown under light microscopy.

Representative Results

The aforementioned surgical procedures lasted from 45 to 60 min. Ostectomy and osteosynthesis were easy to perform with the help of a surgeon's assistant but without using any magnifying system. No intraoperative complications occurred. In a preliminary study on 18 mice[11], postoperative radiographs provided evidence that the bone defect length (3.43 ± 0.12 mm) and the plate positioning (distance between the stifle joint cavity and the distal part of plate = 2.65 ± 0.56 mm) were reproducible.

The anesthesia-related mortality rate was about 5%.

Functional recovery of the operated limb was excellent in all animals and full weight-bearing was observed within a day after surgery **(Animated Figure 1)**. The weight of the osteosynthesis (plate and screws) used in the present study was about 0.1% of the mouse body weight. No postoperative complications (*e.g.,* wound infection, implant failure, bone graft migration, *etc.*) occurred. No self-injury or injuries caused by cagemates occurred.

When the surgically-induced bone defects were left empty, no significant bone formation was observed with consistent bone non-union. In contrast, when the defects were filled with either an isograft or a coral scaffold, newly-formed bone extending from the proximal and distal bone edges was observed. In addition, whereas bone formation allowed re-establishment of bone continuity in most defects treated with isografts **(Figure 8)**, it was only observed inside the coral scaffold in defects filled with this material. In fact, no bone was observed at a distance greater than 1 mm from the bony edges. Absence of cartilage in all histological analyses results provided evidence of the stability of the achieved osteosynthesis **(Figure 9, Figure 10)**.

Radiographs and microCT analyses provided evidence that bone union did not occur in any animal of the defect-left-empty group, 10 weeks post implantation. The volume of mineralized tissue assessed by microCT analyses was 0.8 ± 0.3 mm^3 and was representative of the newly formed-bone. In the isograft and coral scaffold groups, bone union was obtained in 4 and 4 animals respectively. The volume of mineralized tissue assessed by microCT analyses was 4.4 ± 0.9 mm^3 and 8.9 ± 0.7 mm^3. In these groups, however, because both the isograft and the coral scaffold contained minerals, new bone formation could not be truly distinguished from the remaining implanted material (isograft or coral scaffold). Both the rate of bon union and the volume of mineralized tissue obtained from the isograft group and from the coral scaffold group were significantly ($p < 0.001$) higher than those obtained from the defect-left-empty group.

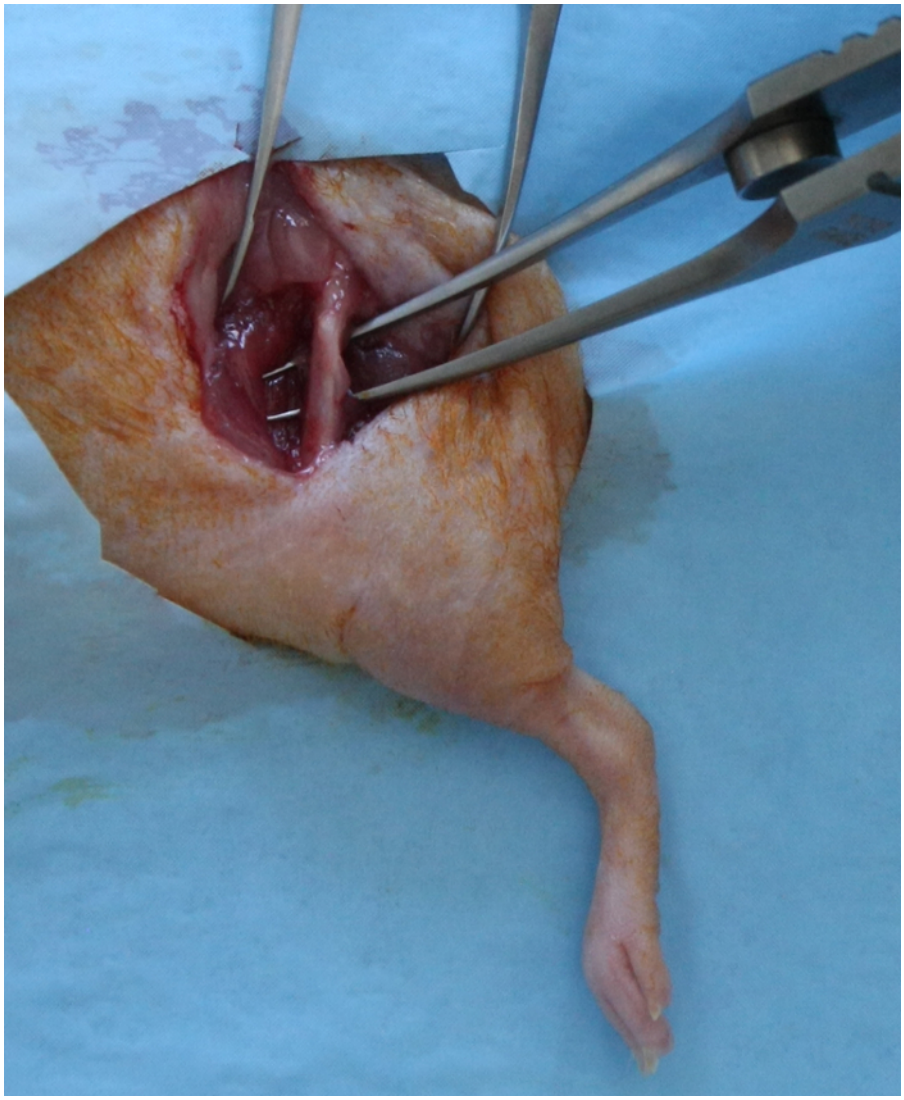

Figure 1: Surgical Exposure for Creation of the Femoral Segmental Defect. A 15 - 17-mm longitudinal skin incision, extending from the hip joint to the stifle joint, was made over the anterolateral aspect of the femur. The *fascia lata* was incised; the *vastus lateralis* muscle and the *biceps femoris* muscle were split to expose the full length of the femoral diaphysis. Please click here to view a larger version of this figure.

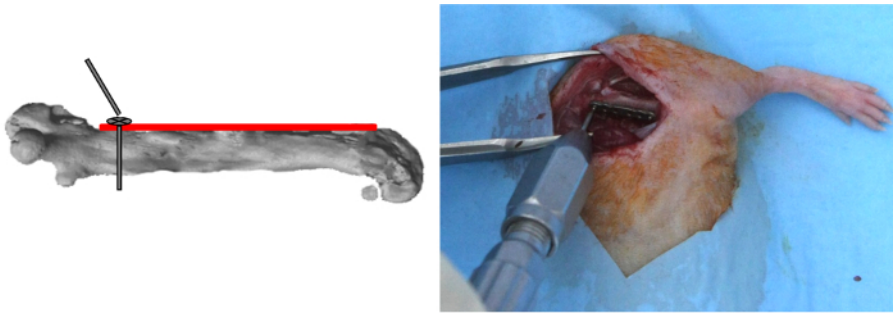

Figure 2: Plate Positioning and Proximal Screw Placement. The plate was applied on the anterior femoral side. The most proximal hole of the plate was drilled; the first screw was inserted and, then, locked. Please click here to view a larger version of this figure.

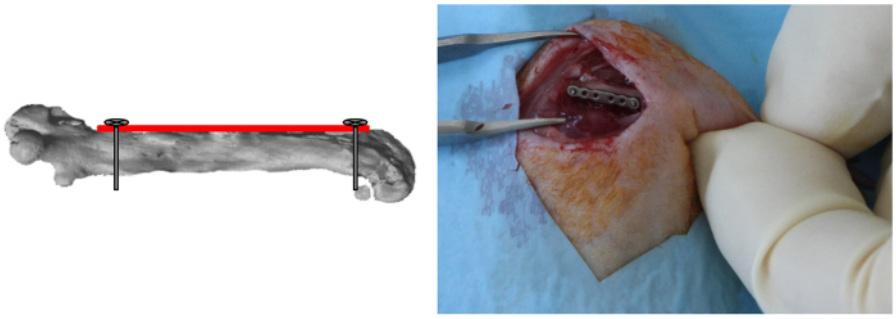

Figure 3: Distal Screw Placement. The most distal hole of the plate was drilled and the screw was inserted and locked. (Reprinted with permission from Tissue Eng Part C, 2013, 19(4), 271-280) Please click here to view a larger version of this figure.

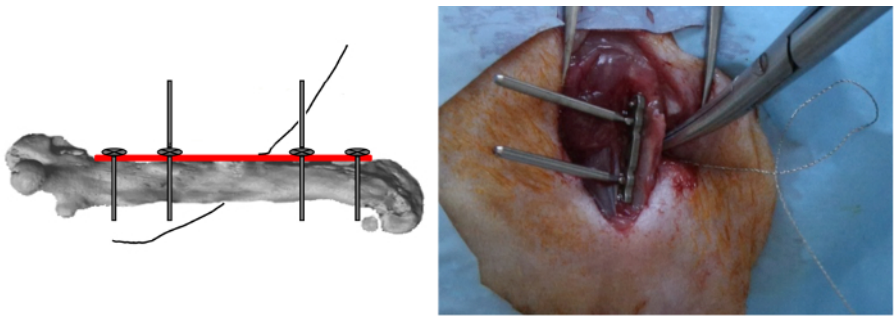

Figure 4: Gigli Saw Positioning. The two other outer screws were inserted but not locked and the wire of the 0.22 mm Gigli saws was tied closely around the bone in a medio-lateral orientation. Please click here to view a larger version of this figure.

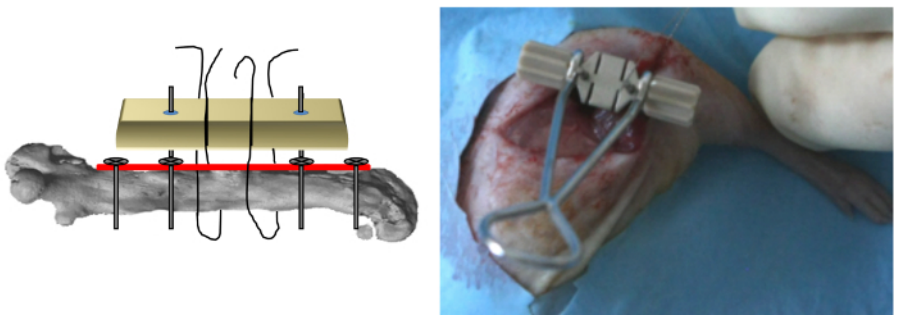

Figure 5: Jig Positioning. The jig was inserted on the stem of the two last screws and applied above the plate and the wire of the saw was then inserted in the slots of the jig. (Reprinted with permission from Tissue Eng Part C, 2013, 19(4), 271-280) Please click here to view a larger version of this figure.

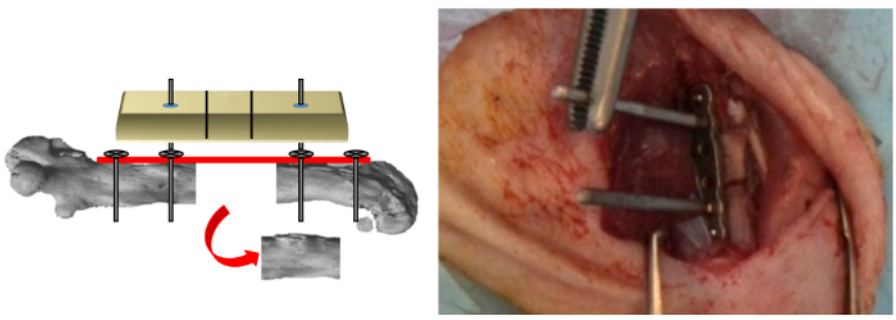

Figure 6: Ostectomy. Ostectomy was performed and the Gigli saw was withdrawn. (Reprinted with permission from Tissue Eng Part C, 2013, 19(4), 271-280) Please click here to view a larger version of this figure.

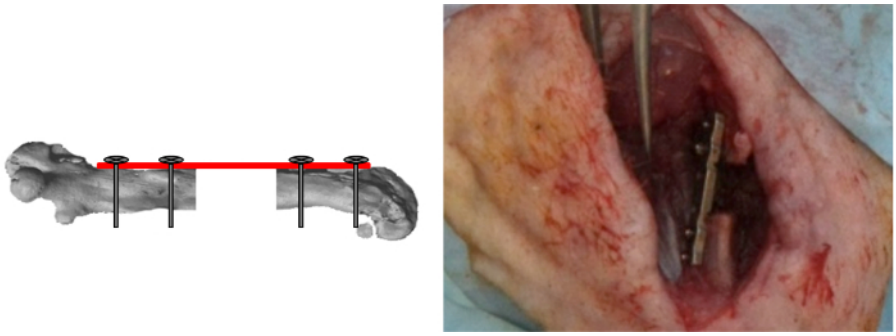

Figure 7: Inner Screws Locking. The jig was removed and the two last screws locked. The segmental defects were then either left empty or filled with the materials tested. (Reprinted with permission from Tissue Eng Part C, 2013, 19(4), 271-280) Please click here to view a larger version of this figure.

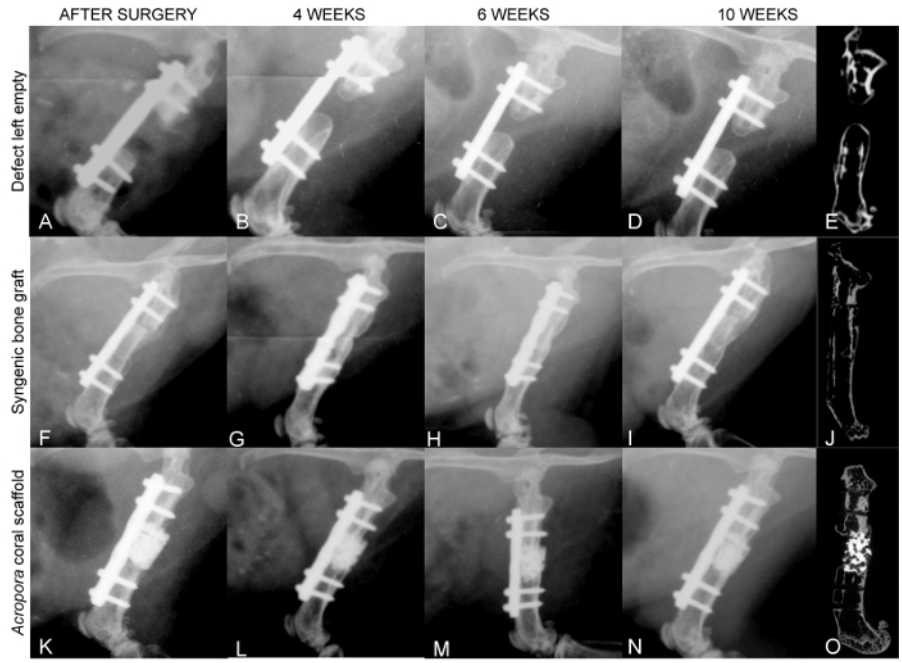

Figure 8: Representative Postoperative Radiographs and Sagittal µCT Reconstruction of the Femoral Bone of Mice. Femoral bone with the respective defect either left empty **(A-E)**, or filled with massive syngenic bone graft **(F-J)**, or filled with massive *Acropora* coral scaffolds **(K-O)**; immediately after surgery **(A, F, K)**, 4 weeks after surgery **(B, G, L)**, 6 weeks after surgery **(C, H, M)**, and 10 weeks after surgery **(D, E, I, J, N, O)** (plate length = 10 mm). (Reprinted with permission from Tissue Eng Part C, 2013, 19(4), 271-280) Please click here to view a larger version of this figure.

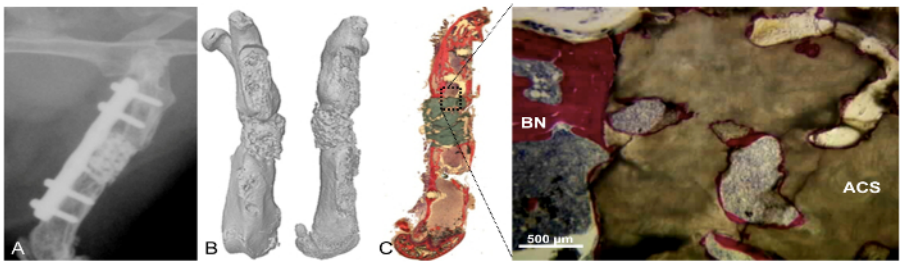

Figure 9: Representative Radiograph, µCT Reconstruction and Histology of a Defect Filled with the Coral Scaffold Tested in the Present Study. A large amount of newly formed bone was observed in-between the surrounding bony edges and the coral scaffold; in contrast, little bone was present inside the scaffold. Stains: Stevenel Blue and von Gieson picrofuchsin. Under these conditions, bone, cells, and coral stained red, blue, and brown, respectively. Scale bar = 500 µm. ACS = *Acropora* coral scaffold; BN = bone. (Reprinted with permission from Tissue Eng Part C, 2013, 19(4), 271-280) Please click here to view a larger version of this figure.

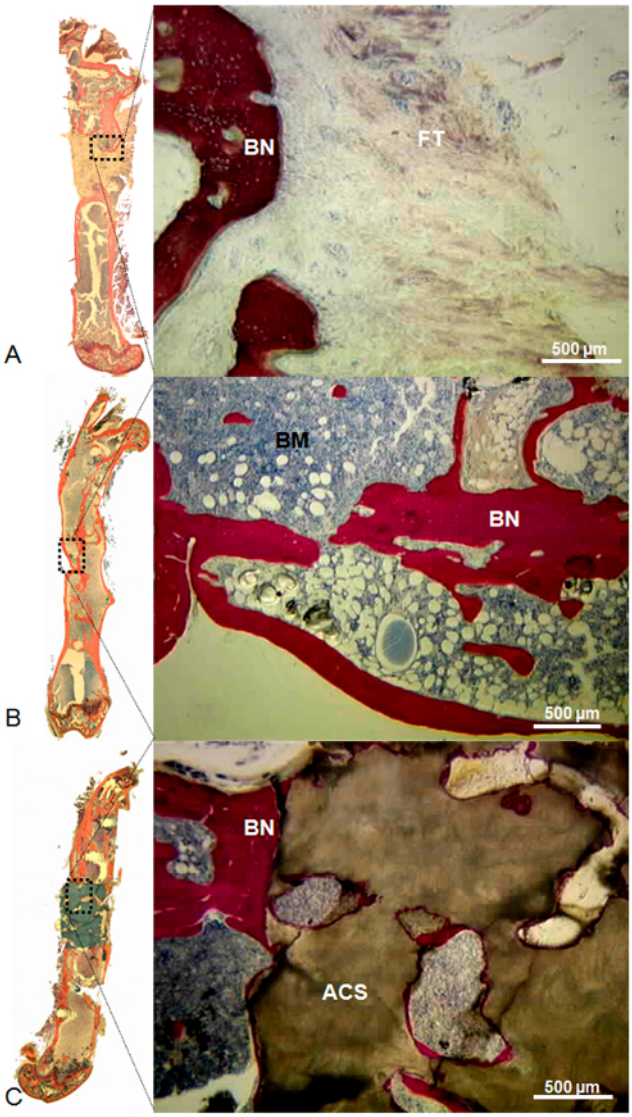

Figure 10: Representative Histology of a Defect Left Empty (A), Filled with Massive Syngenic Bone Graft (B), and Filled with Coral Scaffold (C). In the defect left empty, rounding of the bony edges with medullary canal filling and abundant fibrous tissue deep into the defect were observed. In the defect filled with massive syngenic bone graft, bone continuity was observed between the graft and the surrounding bony edges; bone marrow was present throughout the original cavity. In the defect filled with coral scaffold, newly formed bone was observed between the surrounding bony edges and the coral scaffold, but little bone was present inside the scaffold. Stains: Stevenel Blue and von Gieson picrofuchsin. Under these conditions, bone, cells, and coral stained red, blue, and brown, respectively. Scale bar = 500 mm. ACS, coral scaffold; BN, bone; BM, bone marrow; FT, fibrous tissue.(Reprinted with permission from Tissue Eng Part C, 2013, 19(4), 271-280) Please click here to view a larger version of this figure.

Animated/video Figure 1: Representative video of the gait of a mouse one day postoperative. Full weight bearing was observed. Please click here to view this video.

Discussion

Ectopic implantation of orthopaedic-related materials and device in mice is commonly performed to assess the bone forming capacities of various scaffolds[13,14]. Important differences however exist between ectopic and orthotopic models, including native osteogenic signaling factors and paracrine interactions with host bone-forming cells.

The present study establishes a reproducible murine large segmental, critical-size femoral defect (3.5 mm, approximately 20-25% of the femur length). Considering the size of such defect and the stability provided by the resultant plate osteosynthesis, this model mimics the clinically-encountered atrophic bone non-union.

The post-operative time period chosen in the present study, is in line with previously described non-union models mice, showing a lack of adequate healing after 8 to 12 weeks[4,9,15,16].

Most importantly, reproducible and stable osteosynthesis, as well as stability of the implanted bone substitutes were obtained without significant morbidity and mortality[1,2] with the use of both locking plate and a jig to perform the ostectomy. This outcome contrasts also the results reported when either an external fixator or an intramedullary nail were used [4,5,17-24]. For the external fixators potential disadvantages include: variability in stiffness, infections of the pins tracts, loosening of the pins, potentials injuries due to the pins and the weight of the materials (4 to 20% of the mouse body weight). For the intramedullary nail potential disadvantages include: filling of the medullary cavity with the nail and iatrogenic damage of the articular surfaces.

Other murine segmental, critical-size femoral defects stabilized by plate osteosynthesis have been described with bone defect created by a burr and ranging from 1.5 to 2-mm length[16,25]. In the present model, the use of a jig and a saw wire allowed a precise 3.5 mm-long ostectomy without significant muscles trauma.

However, to succeed in performing the procedure one should take on consideration several key points: Do not use small mice (Nude mice with either a weight under 25 g or age under 8 weeks) otherwise the plate should be too long. When approaching the femoral bone, take care to preserve both the sciatic nerve caudally and the articular capsule distally. Apply the plate on the anterior side of the femoral bone and since alignment of the plate is determined by application of this first screw, take care to position the plate parallel to the femur when inserting this first screw.

Before making the ostectomy, take care to perform a circular dissection of the femur at the middle of the diaphysis to avoid muscular trauma. When performing the ostectomy, the surgeon's assistant must hold firmly the guide and the surgeon must be careful (i) not to tangle the saw wire, (ii) to use the middle two-thirds of the wire while applying a constant steady tension, and (iii) to avoid excess movement to obtain a straight bone cut.

Bone healing is possible in the present model provided a bone graft is used. Moreover, this model allows further studies of the mechanisms involved in bone replacement strategies when either human-origin grafts or cells are used in a well-standardized, large, segmental, bone defect.

In addition, in line to current trends requiring refinement and reduction of use of animals in orthopedics-related research, this model can be used in conjunction with *in vivo* imaging techniques such as bioluminescence. Such non-invasive techniques allow monitoring both implanted cell survival and tissue healing without requiring animal sacrifice [26].

Major limitations of the present model are both the load-bearing conditions and the volume of the bone defect created because they do not fully mimic those encountered clinically in humans. Other limitations of the model are (i) the radio-opacity of the plate which may require removal of the plate before *ex vivo* µCT analysis and may complicate interpretation of the longitudinal radiographic examination results and, (ii) the inability to modulate plate stiffness which may be a key mechanical parameter in bone formation[27-30].

One must keep in mind also, when using either bone isograft or other scaffolds containing a mineral component (specifically calcium carbonate), that some bias are introduced in the segmentation process of the micro-CT analysis, because newly-formed bone density partly overlapped with either the isograft density or scaffold density. For this reason the bone volume obtain by the micro-CT analysis mostly reflect the volume of mineralized tissue (newly-formed bone plus bone substitute)[11,26,31].

Disclosures

The authors declare that they have no competing financial interests.

Acknowledgements

The authors wish to thank Rena Bizios for her valuable comments on the manuscript.

References

1. Auer, J. A. *et al.* Refining animal models in fracture research: seeking consensus in optimising both animal welfare and scientific validity for appropriate biomedical use. *BMC Musculoskelet Disord.* **8**), 72 (2007).
2. Histing, T. *et al.* Small animal bone healing models: standards, tips, and pitfalls results of a consensus meeting. *Bone.* **49** (4), 591-599 (2011).
3. Horner, E. A. *et al.* Long bone defect models for tissue engineering applications: criteria for choice. *Tissue Eng. Part B Rev.* **16** (2), 263-271 (2010).
4. Srouji, S. *et al.* A model for tissue engineering applications: femoral critical size defect in immunodeficient mice. *Tissue Eng. Part C Methods.* **17** (5), 597-606 (2011).
5. Thompson, Z., Miclau, T., Hu, D., Helms, J. A. A model for intramembranous ossification during fracture healing. *J Orthop Res.* **20** (5), 1091-1098 (2002).
6. Harris, J. S., Bemenderfer, T. B., Wessel, A. R., Kacena, M. A. A review of mouse critical size defect models in weight bearing bones. *Bone.* **55** (1), 241-247 (2013).
7. Garcia, P. *et al.* The LockingMouseNail--a new implant for standardized stable osteosynthesis in mice. *J. Surg. Res.* **169** (2), 220-226 (2011).
8. Garcia, P., Histing, T., Holstein, J. H., Pohlemann, T., Menger, M. D. Femoral non-union models in the mouse. *Injury.* **41** (10), 1093-1094 (2010).
9. Garcia, P. *et al.* Development of a reliable non-union model in mice. *J. Surg. Res.* **147** (1), 84-91 (2008).
10. Viateau, V., Logeart-Avramoglou, D., Guillemin, G., Petite, H. Animal Models for bone tisue enginering purposes. In: *Sourcebook of models for biomedical research.* Conn, P.M., eds., Humana Press, 725-738 (2008).
11. Manassero, M. *et al.* A novel murine femoral segmental critical-sized defect model stabilized by plate osteosynthesis for bone tissue engineering purposes. *Tissue Eng. Part C Methods.* **19** (4), 271-280 (2013).
12. Matthys, R., Perren, S. M. Internal fixator for use in the mouse. *Injury.* (**40 Suppl 4**), S103-109 (2009).
13. Becquart, P. *et al.* Ischemia is the prime but not the only cause of human multipotent stromal cell death in tissue-engineered constructs in vivo. *Tissue Eng. Part A.* **18** (19-20), 2084-2094 (2012).
14. Deschepper, M. *et al.* Proangiogenic and prosurvival functions of glucose in human mesenchymal stem cells upon transplantation. *Stem Cells.* **31** (3), 526-535 (2013).
15. Oetgen, M. E., Merrell, G. A., Troiano, N. W., Horowitz, M. C., Kacena, M. A. Development of a femoral non-union model in the mouse. *Injury.* **39** (10), 1119-1126 (2008).
16. Liu, K. *et al.* A murine femoral segmental defect model for bone tissue engineering using a novel rigid internal fixation system. *J Surg Res.* **183** (2), 493-502 (2013).
17. Zwingenberger, S. *et al.* Establishment of a femoral critical-size bone defect model in immunodeficient mice. *J Surg Res.* **181** (1), e7-e14 (2013).
18. Cheung, K. M. *et al.* An externally fixed femoral fracture model for mice. *J. Orthop Res.* **21** (4), 685-690 (2003).
19. Claes, L. *et al.* Hyperhomocysteinemia is associated with impaired fracture healing in mice. *Calcif. Tissue Int.* **85** (1), 17-21 (2009).
20. Drosse, I. *et al.* Validation of a femoral critical size defect model for orthotopic evaluation of bone healing: a biomechanical, veterinary and trauma surgical perspective. *Tissue Eng. Part C Methods.* **14** (1), 79-88 (2008).
21. Holstein, J. H. *et al.* Advances in the establishment of defined mouse models for the study of fracture healing and bone regeneration. *J. Orthop. Trauma.* **23** (5 Suppl), S31-38 (2009).
22. Johnson, K. D., August, A., Sciadini, M. F., Smith, C. Evaluation of ground cortical autograft as a bone graft material in a new canine bilateral segmental long bone defect model. *J. Orthop. Trauma.* **10** (1), 28-36 (1996).
23. Meinig, R. P., Buesing, C. M., Helm, J., Gogolewski, S. Regeneration of diaphyseal bone defects using resorbable poly(L/DL-lactide) and poly(D-lactide) membranes in the Yucatan pig model. *J. Orthop. Trauma.* **11** (8), 551-558 (1997).
24. Wu, J. J., Shyr, H. S., Chao, E. Y., Kelly, P. J. Comparison of osteotomy healing under external fixation devices with different stiffness characteristics. *J. Bone Joint Surg. Am.* **66** (8), 1258-1264 (1984).
25. Xing, J. *et al.* Establishment of a bilateral femoral large segmental bone defect mouse model potentially applicable to basic research in bone tissue engineering. *J. Surg. Res* **192** (2), 454-463 (2014).
26. Manassero, M. *et al.* Comparison of Survival and Osteogenic Ability of Human Mesenchymal Stem Cells in Orthotopic and Ectopic Sites in Mice. *Tissue Eng. Part A.* **22** (5-6), 534-544 (2016).
27. Bos, R. R. *et al.* Degradation of and tissue reaction to biodegradable poly(L-lactide) for use as internal fixation of fractures: a study in rats. *Biomaterials.* **12** (1), 32-36 (1991).
28. Oest, M. E., Dupont, K. M., Kong, H. J., Mooney, D. J., Guldberg, R. E. Quantitative assessment of scaffold and growth factor-mediated repair of critically sized bone defects. *J.Orthop. Res.* **25** (7), 941-950 (2007).
29. Pihlajamaki, H., Bostman, O., Tynninen, O., Laitinen, O. Long-term tissue response to bioabsorbable poly-L-lactide and metallic screws: an experimental study. *Bone.* **39** (4), 932-937 (2006).

30. Rai, B. *et al.* Combination of platelet-rich plasma with polycaprolactone-tricalcium phosphate scaffolds for segmental bone defect repair. *J. Biomed. Mater Res. A* **81** (4), 888-899 (2007).
31. Komlev, V. S. *et al.* Kinetics of in vivo bone deposition by bone marrow stromal cells into porous calcium phosphate scaffolds: an X-ray computed microtomography study. *Tissue Eng*. **12** (12), 3449-3458 (2006).